

Conference Proceedings

1st International Conference on Applied Mineralogy & Advanced Materials - AMAM2015

Effects of Li/Mn mole ratio on the synthesis of $\text{Li}_{1+x}\text{Mn}_{2-x}\text{O}_4$ by low temperature solid-state reaction for cathode materials

Dyah Purwaningsih^{1,2*}, Roto Roto¹, Narsito Muhammad¹, Hari Sutrisno²

¹Department of Chemistry, Faculty of Mathematics and Natural Sciences, Gadjah Mada University Sekip Utara, Yogyakarta 55281, Indonesia

²Department of Chemistry Education, Faculty of Mathematics and Natural Sciences, Yogyakarta State University Kampus Karangmalang, Yogyakarta 55281, Indonesia
*dyahuny@yahoo.com

Abstract

This study aims to determine the effects of the mole ratio of precursor on the synthesis of $\text{Li}_{1+x}\text{Mn}_{2-x}\text{O}_4$ ($x=0; 0.02; 0.04; 0.06; 0.08; 0.1$) by low temperature solid-state reaction. The variable examined in this study was the mole ratio of Li/ Mn in $\text{Li}_{1+x}\text{Mn}_{2-x}\text{O}_4$. The compound was characterized by XRD, SEM-EDS, TEM and FTIR while the microstructural analysis of LiMn_2O_4 was performed by Direct Method using several programs including winPLOT, DICVOL, Checkcell and Diamond using XRD data. It is found that the mole ratio of the precursor affects the size, crystallinity and structure of $\text{Li}_{1+x}\text{Mn}_{2-x}\text{O}_4$. The results shows that $\text{Li}_{1+x}\text{Mn}_{2-x}\text{O}_4$ has a cubic crystal structure with $Fd\bar{3}m$ phase and the increase in the mole precursor causes a change in the material structure of $\text{Li}_{1+x}\text{Mn}_{2-x}\text{O}_4$ into orthorhombic $Fddd$.

Keywords: $\text{Li}_{1+x}\text{Mn}_{2-x}\text{O}_4$; Li/Mn mole ratio; low temperature; solid state reaction.

1. Introduction

Lithium battery has received great attention in research. In addition to having high power, lithium battery is light and can be used multiple times (rechargeable). With the rapid

development of technology, the needs for more capable lithium battery to produce higher energy becomes indispensable (Thackeray, 2004; Armand & Tarascon, 2008; Song, 2011).

The performance, the price and safety of Li-ion batteries mainly depend on the properties of cathode materials. Attention has been paid to the development of high capacity, cheap and safe cathode materials (Ritchie & Howard, 2006). LiMn_2O_4 is very promising candidate because its low cost and safety characteristics are superior compared to layered cobalt or nickel oxides (Aifantis et al., 2010; Manjunatha et al., 2010; Xu et al., 2012). LiMn_2O_4 is quite distinct from such layered oxides in that it is a three-dimensional host. The spinel structure space group $Fd3m$ consists of cubic closed-packed oxide ions Mn ions in one half of the octahedral sites and Li^+ in one eighth of the tetrahedral sites within the cubic close-packed oxide array. The Mn_2O_4 framework of the spinel structure is highly stable, and defines a series of tunnels formed by the face-sharing of tetrahedral lithium (8a) and empty octahedral (16c) sites. These tunnels intersect in three dimensions and support rapid lithium diffusion but, unlike the layered compounds, the spinels are selective for lithium ions over solvent molecules or other larger cations because of their greater structural rigidity (Bruce, 1997; Patil et al., 2008; Julien & Massot, 2003).

There are various approaches to the synthesis of LiMn_2O_4 spinel including conventional solid reaction (Kim et al., 2008; Lee et al., 2010), sol-gel reaction (Lakshmi et al., 1997; Kumar et al., 2003), and Pechini process. Compared to sol-gel and Pechini approaches, in which additional starting materials and synthetic materials and synthetic procedures are generally needed for preparation and separation of the targeted Li-Mn precursors, solid reaction is simpler and easier to handle. Therefore, in this work we used solid reaction to synthesize $\text{Li}_{1+x}\text{Mn}_{2-x}\text{O}_4$ ($x=0; 0.02; 0.04; 0.06; 0.08; 0.10$).

A series of LiMn_2O_4 compounds were prepared using a low temperature solid-state reaction, i.e., reflux technique at various Li/Mn mole ratios. The advantage of this technique is that it can be done for a longer time without the need for adding more solvent or fear of the reaction vessel boiling dry, as the vapour is immediately condensed. In addition, as a given solvent will always boil at a certain temperature, one can be sure that the reaction will proceed at a constant temperature. The effects of the synthetic Li/Mn mole ratio on the structure of the products are to be investigated in details.

2. Experimental section

2.1 Synthesis of MnO_2 and LiMn_2O_4 nanorods

Analytical grade of $\text{Mn}(\text{CH}_3\text{COO})_2$ and $\text{Na}_2\text{S}_2\text{O}_8$ (Aldrich) were used to prepare MnO_2 nanorods by reflux technique. All chemicals were used without further purification. In a typical synthesis, $\text{Mn}(\text{CH}_3\text{COO})_2$ and $\text{Na}_2\text{S}_2\text{O}_8$ were dissolved at room temperature with a molar ratio of 1:1 in 80 mL deionized distilled water by magnetic stirring to form a homogeneous clear solution. The mixed solution was transferred into boiling flask and heated at 120 °C for 12 hours. The obtained powder was subsequently dried at 100 °C for 12 h in air (Purwaningsih et al., 2015).

A typical synthesis of LiMn_2O_4 is as follows: 0.00143 moles of LiOH and 0.0028 moles of as-synthesized MnO_2 were dispersed into 2 mL high purity ethanol to form a thick slurry, ground to form a fine mixture for several hours and dried at room temperature. The above process was repeated two or three times to produce a well-mixed powder. The powder was

then calcined at 750 °C for 5 hours. The same procedure was conducted for $\text{Li}_{1.02}\text{Mn}_{1.98}\text{O}_4$; $\text{Li}_{1.04}\text{Mn}_{1.96}\text{O}_4$; $\text{Li}_{1.06}\text{Mn}_{1.94}\text{O}_4$; $\text{Li}_{1.08}\text{Mn}_{1.92}\text{O}_4$ and $\text{Li}_{1.10}\text{Mn}_{1.90}\text{O}_4$.

2.2 Characterization of $\text{Li}_{1+x}\text{Mn}_{2-x}\text{O}_4$ microstructure

The synthesized MnO_2 and $\text{Li}_{1+x}\text{Mn}_{2-x}\text{O}_4$ ($x = 0, 0.02, 0.04, 0.06, 0.08, \text{ and } 0.10$) nanostructures were characterized using an X-ray diffractometer (XRD Rigaku, Miniflex) with $\text{Cu K}\alpha$ radiation ($\lambda = 0.15406 \text{ nm}$ at 40 kV and 40 mA). Using XRD data, the structural analysis of the products was performed by the Direct Method using several programs that are winPLOTR, DICVOL, Checkcell and Diamond. The size and shape of the nanoparticles were observed by Transmission Electron Microscopy (TEM).

3. Results and discussions

3.1 Structure and morphology of LiMn_2O_4

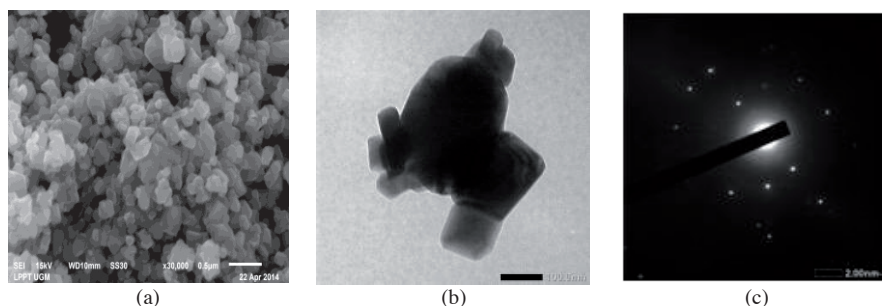


Fig. 1. (a) SEM images (b) TEM images (c) SAED pattern of LiMn_2O_4 .

Single phase spinels with a Li:Mn ratio of 1:2 of composition LiMn_2O_4 are formed around in 750 °C in air. Irrespectively, of the choice of the Li and Mn starting material, nearly black material with a cubic cell and a lattice constant 8.2452 Å are obtained. According to the Scanning Electron Microscopy (SEM) observations, the material is well formed and exhibits clearly developed crystal faces (Fig. 1). The TEM images and selected area of the electron diffraction (SAED) pattern further revealed that LiMn_2O_4 has the high quality cubic (space group $Fd\bar{3}m$) crystalline nanorods with diameter 50-100 nm.

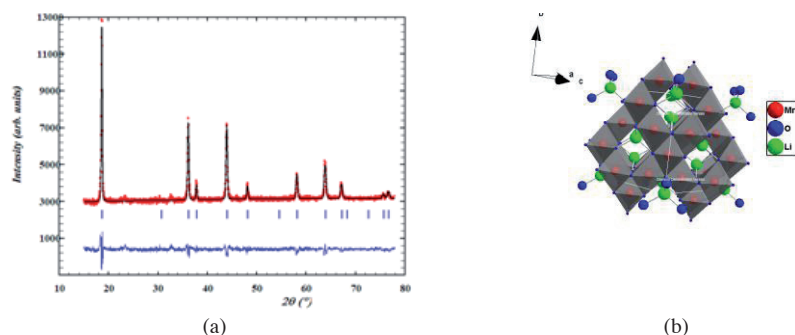


Fig. 2. (a) XRD pattern (b) Microstructure of LiMn_2O_4 .

From the structural calculation using Direct Method, it is showed that LiMn_2O_4 in the space group $Fd\bar{3}m$. This is in agreement with the complete occupation of the site 8a by Li, the site 16d by Mn, and the site 32e by oxygen.

3.2 Structure and morphology of $\text{Li}_{1.02}\text{Mn}_{1.98}\text{O}_4$ and $\text{Li}_{1.04}\text{Mn}_{1.96}\text{O}_4$

The TEM images and SAED pattern further revealed that $\text{Li}_{1.02}\text{Mn}_{1.98}\text{O}_4$ and $\text{Li}_{1.04}\text{Mn}_{1.96}\text{O}_4$ have the high quality cubic (space group $Fd\bar{3}m$) crystalline nanorods. The nanorods were well-dispersed and one-dimensional with an average diameter between 50-100 nm. The corresponding SAED pattern supports the formation of structure of cubic crystalline nanorods.

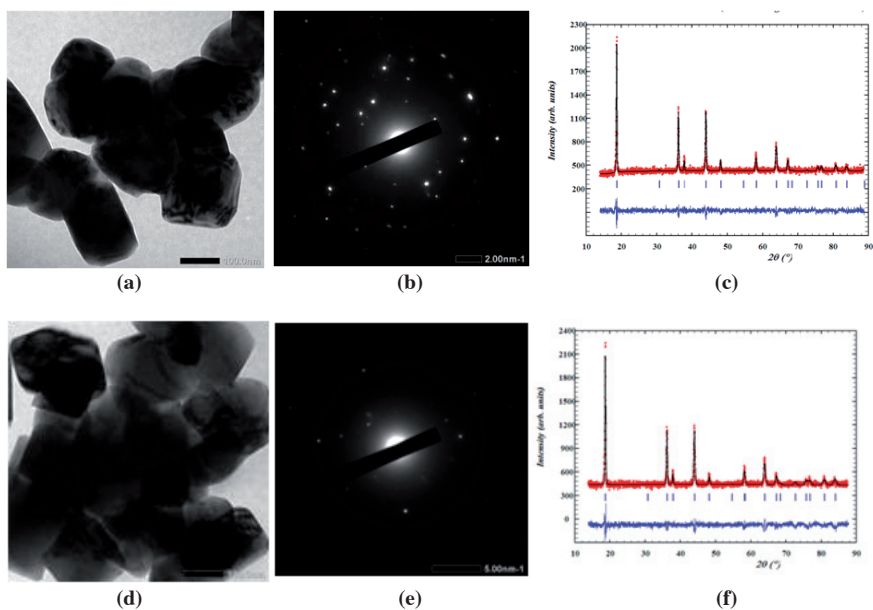


Fig. 3. (a) TEM images (b) SAED pattern (c) XRD pattern of $\text{Li}_{1.02}\text{Mn}_{1.98}\text{O}_4$ (d) TEM images (e) SAED pattern (f) XRD pattern of $\text{Li}_{1.04}\text{Mn}_{1.96}\text{O}_4$.

3.3 Structure and morphology of $\text{Li}_{1.06}\text{Mn}_{1.94}\text{O}_4$, $\text{Li}_{1.08}\text{Mn}_{1.92}\text{O}_4$ and $\text{Li}_{1.10}\text{Mn}_{1.90}\text{O}_4$

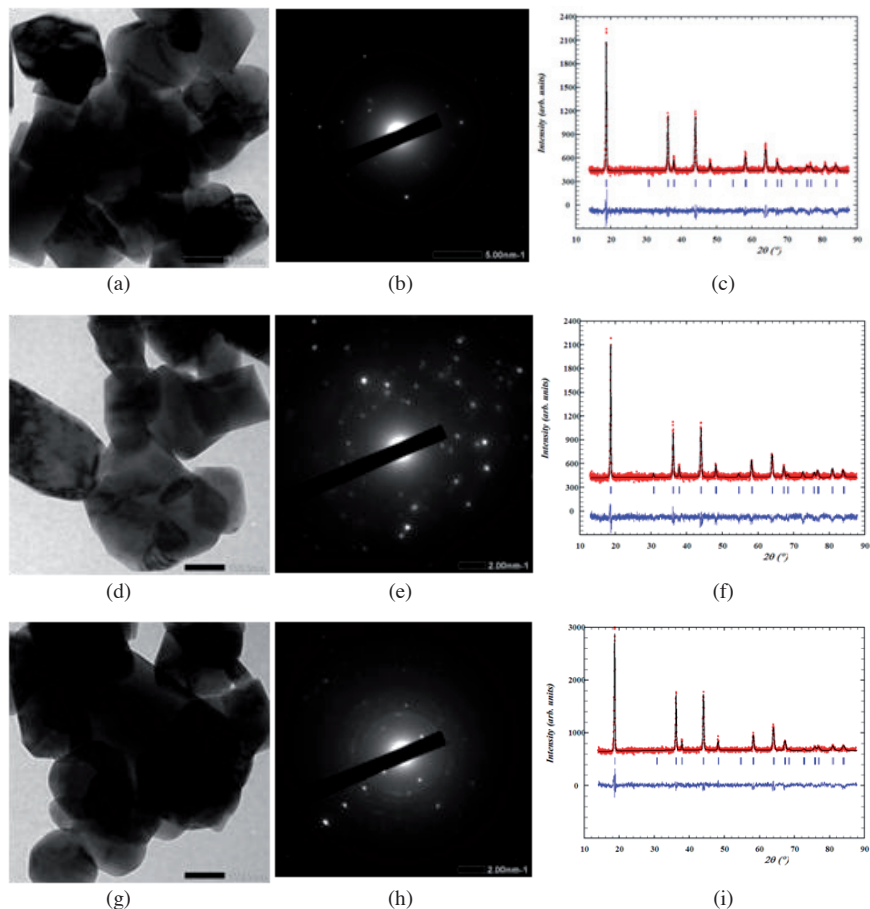


Fig. 4. (a) TEM images (b) SAED pattern (c) XRD pattern of $\text{Li}_{1.06}\text{Mn}_{1.94}\text{O}_4$ (d) TEM images (e) SAED pattern (f) XRD pattern of $\text{Li}_{1.08}\text{Mn}_{1.92}\text{O}_4$ (g) TEM images (h) SAED pattern (i) XRD pattern of $\text{Li}_{1.10}\text{Mn}_{1.90}\text{O}_4$.

The TEM images and SAED pattern further revealed $\text{Li}_{1.06}\text{Mn}_{1.94}\text{O}_4$, $\text{Li}_{1.08}\text{Mn}_{1.92}\text{O}_4$ and $\text{Li}_{1.10}\text{Mn}_{1.90}\text{O}_4$ have the high quality orthorhombic (space group $Fddd$) crystalline. The nanorods were well-dispersed and maintained one-dimensional with an average diameter between 50-100 nm. The corresponding SAED pattern supports the formation structure of orthorhombic $Fddd$ crystalline nanorods.

Table 1. Lattice parameter, volume and agreement factor of $\text{Li}_{1+x}\text{Mn}_{2-x}\text{O}_4$.

Variation x	Space Group	a	b	c	v	Rp	Rwp	Re	Chi ²
0	Cubic $Fd\bar{3}m$	8.245200	8.245200	8.245200	560.5259	33.4	18.9	11.8	2.560
0.02	Cubic $Fd\bar{3}m$	8.242592	8.242592	8.242592	560.0044	76	32.6	35.9	0.914
0.04	Cubic $Fd\bar{3}m$	8.230799	8.230799	8.230799	557.6041	60.7	35.9	28.1	1.639
0.06	Orthorhombic $Fddd$	8.234879	8.232482	8.234783	558.2647	69.4	32	32.5	0.967
0.08	Orthorhombic $Fddd$	8.229085	8.233565	8.233167	557.8358	76.3	38.2	33.2	1.320
0.1	Orthorhombic $Fddd$	8.230813	8.224436	8.225409	556.8091	59.5	27.3	27.8	0.964

From the analysis using FullProf Pattern Matching, it is seen that the stoichiometric ratio of the change in structural changes in the system Li-Mn-O of the *Fd3m* cubic phase into orthorhombic *Fddd*. These changes result from the Jahn-Teller distortion effects caused by Mn^{3+} ions. It is possible that Mn^{3+} ions replaced by Li^+ ions.

4. Conclusions

$Li_{1+x}Mn_{2-x}O_4$ ($x=0; 0.02; 0.04; 0.06; 0.08; 0.10$) have been prepared and characterized using low temperature solid-state reaction. The results shows that $Li_{1+x}Mn_{2-x}O_4$ ($x=0; 0.02$ and 0.04) have a cubic crystal structure with space group of *Fd3m* and the increase in the mole precursor causes a change in the material structure of $Li_{1+x}Mn_{2-x}O_4$ ($x=0.06; 0.08; 0.10$) into orthorhombic *Fddd*.

References

- Thackeray M.M. (2004). Batteries, Transportation applications, 127-139.
- Armand M., Tarascon J.M. (2008). Building better batteries. *Nature* 451, 652-657.
- Song M.K., Park S., Alamgir F.M., Cho J., Liu M. (2011). Nanostructured electrodes for lithium-ion and lithium-air batteries: the latest developments, challenges, and perspectives. *Material Science Engineering Reports* 72, 203-252.
- Ritchie A., Howard W. (2006). Recent developments and likely advances in lithium-ion batteries. *Journal of Power Sources* 162, 809-812.
- Aifantis K.E., Hackney S.A., Kumar R.V. (2010). *High Energy Density Lithium Batteries*. Weinheim, Germany: Wiley-VCH Verlag GmbH & Co. KGaA.
- Manjunatha H., Suresh G.S., Venkatesha T.V. (2010). Electrode materials for aqueous rechargeable lithium batteries. *Journal of Solid State Electrochemistry* 15, 431-445.
- Xu B., Qian D., Wang Z., Meng Y.S. (2012). Recent progress in cathode materials research for advanced lithium ion batteries. *Material Science Engineering Reports* 73(5-6), 51-65.
- Bruce G.P. (1997). Solid-state chemistry of lithium power sources. *Chemical Communication* 19, 1817-1824.
- Patil A., Patil V., Wook S.D., Choi J.W., Paik D.S., Yoon S.J. (2008). Issue and challenges facing rechargeable thin film lithium batteries. *Materials Research Bulletin* 43, 1913-1942.
- Julien C.M., Massot M. (2003). Lattice vibrations of materials for lithium rechargeable batteries I. Lithium manganese oxide spinel. *Materials Science Engineering* 97, 217-230.
- Kim D.K., Muralidharan P., Lee H.W., Ruffo R., Yang Y., Chan C.K., Peng H., Huggins R.A., Cui Y. (2008). Spinel $LiMn_2O_4$ nanorods as lithium ion battery cathodes. *Nano Letters* 8, 3948-3952.
- Lee H.W., Muralidharan P., Ruffo R., Mari C.M., Cui Y., Kim D.K. (2010). Ultrathin spinel $LiMn_2O_4$ nanowires as high power cathode materials for Li-ion batteries. *Nano Letters* 10, 3852-3856.
- Lakshmi B.B., Patrissi C.J., Martin C.R. (1997). Sol-gel template synthesis of semiconductor oxide micro- and nanostructures. *Chemistry of Materials* 9, 2544-2550.
- Kumar V.G., Gnanara J.S., David S.B., Pickup D.M., van-Eck E.R.H., Gedanken A., Aurbach D. (2003). An aqueous reduction method to synthesize spinel $LiMn_2O_4$ nanoparticles as a cathode material for rechargeable lithium-ion batteries. *Chemistry of Materials* 15, 4211-4216.
- Purwaningsih D., Roto R., Narsito M., Sutrisno H. (2015). Preparation of $LiMn_2O_4$ microstructure by low temperature solid state reactions for cathode materials. *Advanced Materials Research* 1101, 134-137.